Journal of Ceramic Processing Research. Vol. 26, No. 6, pp. 1111~1121 (2025)
(Received 14 July 2025, Received in revised form 13 September 2025, Accepted 3 October 2025)
https://doi.org/10.36410/jcpr.2025.26.6.1111

J O U R N A L O F
Ceramic Processing Research

The effect of yttrium-containing solutions ($Y(NO_3)_3$ and YCl_3) on the properties of vacuum-impregnated, 3D printed silica ceramics

Xiaoli Shi[a], He Li[a,*], Yunzhi Huang[a] and Paolo Colombo[b]
[a]*Xinjiang Environmental and Functional Materials Engineering Research Center, School of Materials Science and Engineering, Xinjiang University, Urumqi, Xinjiang, 830046, PR China*
[b]*Department of Industrial Engineering, University of Padova, Padova 35131, Italy*

Silica ceramics have attracted much attention due to their excellent mechanical properties, as well as potential applications in different industrial fields. At present, the research on how to improve silica ceramics has been very extensive, with a special focus on thermal for porous components. Therefore, it is useful to find a universally applicable method to improve the mechanical properties of high porosity silica ceramics. In this study, vacuum impregnation technology was used to modify 3D printed silica ceramics, and the effects of two yttrium-containing solutions ($Y(NO_3)_3$ and YCl_3) with different contents on the properties of DLP printed silica ceramics were studied. It was found that NO_3^- present in the $Y(NO_3)_3$ solution is harmless to silica ceramics, while the presence of Cl^- in YCl_3 solution will lead to defects. Therefore, 0.030 mol/L $Y(NO_3)_3$ solution was the best choice for vacuum impregnation of silica ceramics, providing the best microstructure and mechanical properties. In particular, the open porosity of the samples was 26.35 ± 0.13 vol%, the linear shrinkage 4.59 ± 0.15%, the bulk density 1.592 ± 0.006 g/cm^3, and the flexural strength at room temperature 4.51 ± 0.15 MPa, making the 3D printed parts of interest as casting cores for turbine blades.

Keywords: Silica ceramics, Yttrium, Vacuum impregnation, 3D printing, Porous ceramics.

Introduction

Silica ceramics have attracted much attention in various industrial fields due to their excellent mechanical properties, low production costs, and outstanding thermal, optical and other functional properties [1, 2]. Traditional molding techniques, such as gel casting, injection molding and hot pressing, all have the drawbacks of long production cycles and high manufacturing costs, which greatly limit the wide industrial application of silica-based ceramic cores [3-5]. As a type of 3D printing technology, digital light processing (DLP) has the advantage of high precision, short development cycle, low manufacturing cost, less material waste and unlimited design freedom [6, 7]. However, the layer-by-layer manufacturing method of 3D printing leads to a relatively weak bonding force between material layers, thereby reducing the mechanical strength of the printed product [8-10]. In particular, many applications of silica ceramics, such as ceramic cores, catalyst carriers, etc., require high porosity and therefore issues concerning the strength of the parts have to be considered [11-14]. At present, the research on how to improve silica ceramics is very extensive, and the research on porous silica is more focused on thermal [15, 16]. Therefore, it is necessary to find a universally applicable method to enhance the mechanical properties of silica ceramics with high porosity.

Numerous studies have shown that adding a small amount of functional elements is beneficial for improving the mechanical properties of ceramic materials [17, 18]. However, adding sintering aid powder directly during the slurry preparation process may sometimes affect the viscosity of the slurry. When the slurry viscosity is too high, the printing accuracy will be affected. The vacuum impregnation method is a process technology that uses vacuum technology to infiltrate liquid substances into the interior of porous materials. It extracts the gas and air inside the material through vacuum, and then fills the material pores with liquid under pressure or vacuum, thereby introducing functional elements in the liquid substances, thereby improving the performance of the material or meeting certain functional requirements. Due to the high porosity and high specific surface area of porous silica ceramics, the vacuum impregnation process can effectively introduce additives [19-22]. Vacuum conditions are the sole requirement for implementing this mass transfer method, which enhances the mass transfer efficiency without incurring excessive additional costs, and shortens the processing time and production cycle [23-25]. Therefore, vacuum impregnation, as a post-treatment method, has great potential in improving

*Corresponding author:
Tel : 008615210896919
E-mail: lihe@xju.edu.cn

the mechanical properties of ceramics [26-28]. Zheng et al. [12] used LPBF technology to print the green body, and then infiltrated the green body with a silica sol to successfully improve the flexural strength of silica-based ceramic cores. Zhang et al. [20] prepared $ZrSiO_4$ reinforced silica-based ceramic core by enhancing the percolation effect through pre-sintering. Liu et al. [21] improved the microstructure and properties of silica-based ceramic cores by using $Al(OH)_3$ as a mineralizer, combined with vacuum impregnation. A large number of experiments have proved that vacuum impregnation technology can improve the flexural strength of silica-based ceramic cores.

As a dopant, Y_2O_3 can reduce the activation energy of crystal growth, promote the formation and growth of crystals, and improve the density of ceramics [29, 30]. The addition of yttrium elements has been extensively studied in other ceramic systems. Zhang et al[31]. found that the introduction of Y_2O_3 effectively improved the wet oxidation resistance of SiC and SiC_f/SiC composites. Yu et al. [32]. found that Y_2O_3/Hf co-doping can promote the preferential formation of α-alumina by inhibiting the formation of interfacial pores. However, Cheng et al. [33] pointed out, in the study of Al_4SiC_4 ceramics, that excessive Y_2O_3 content resulted in increased porosity and decreased mechanical properties. This is because the addition of Y_2O_3 accelerates the growth of Al_4SiC_4 grains. Excessive Y_2O_3 content can lead to grain coarsening, resulting in uneven phase distribution within the sample, causing stress concentration, and ultimately reducing the mechanical properties of the material. In addition, the powder will form clusters during the dissolution process of casting cores, affecting the effect of impregnation [34, 35]. Therefore, in this study, yttrium-containing solution with lower concentration was selected as the vacuum impregnation material.

In this study, two yttrium-containing solutions ($Y(NO_3)_3$ and YCl_3) with different concentrations were used to study the effect of vacuum impregnation on the properties of DLP printed alumina ceramics. The effects of the two acidic yttrium-containing solutions on the mechanical properties and microstructure of silica ceramics were compared, and an optimal process parameter was selected to provide reference and support for the subsequent application as casting cores.

Experimental

Preparation of raw material

Green bodies were prepared by mixing silica powder and a photosensitive resin. The main components of the photosensitive resin used consist of 5-ethyl-1,3-dioxy-5 (CTFA), 2,4,6-trimethylbenzoyl diphenylphosphine oxide (TPO) and trimethylacrylyl triacrylate (TMPTA). After manually mixing the ceramic powder and photosensitive resin evenly, a table high speed vibrating ball mill (China Hefei Kejing Material Technology Co., Ltd.) was used to ball mill the suspension for 1 hour at a speed of 400 RPM. A green body with a size of 5054 mm was obtained using a DLP 3D printer (Tendimensional Technology Co., Ltd., China). The layer thickness was set to 75 μm and the single layer exposure time was 2 seconds. The print model was drawn by 3ds Max software and sliced using the software that comes with the printer (10dim software).

By adding deionized water to dissolve solid reagents, $Y(NO_3)_3$ (Chengdu Aikeda Chemical Reagent Co., LTD., China) and YCl_3 (Chengdu Aikeda Chemical Reagent Co., LTD., China) were prepared into solutions with different concentrations (0.005, 0.010, 0.015, 0.020, 0.025, 0.030 mol/L).

Sample preparation

The resin used in printing makes the green body hydrophobic and inhibits the solution from penetrating into the green body [20]. At the same time, the porosity of the green body is low, which is not conducive to the penetration of the solution. In order to improve the penetration effect, the green body was first sintered. The sintered samples are not only hydrophilic, but also have high porosity, which is conducive to the diffusion of vacuum impregnation solution [20]. The processing steps for obtaining the green body were as follows: First, the sample was heated to 600 °C at a heating rate of 2 °C/min, and maintained at this temperature for 2 h. The sample was then heated to the target temperature (T=1250 °C) at a heating rate of 5 °C/min and left for 2 h. Finally, the sample was cooled to 600 °C at a heating rate of 5 °C/min, and then cooled to room temperature. This sintering process has been proved appropriate by previous studies [26, 27, 34].

The sintered sample was impregnated in vacuum using different impregnating solutions ($Y(NO_3)_3$, YCl_3). Three different concentrations of solution were used to impregnate at 0.015 MPa in a vacuum drying oven (DFZ vacuum drying oven of Beijing Everbright Medical Equipment Co., Ltd.) for 1.5 h, and the impregnated ceramic sample was re-sintered according to the previously described heating cycle.

Characterization and testing

The microstructure morphology of sintered silicon ceramics was obtained by observing them under a microscope(Helios G4 CX microscope, FEI Corporation). COMSOL software was used to simulate the diffusion of yttrium, and the material parameters used were the ones stored in the software database. The data of the model are based on the software's own material library and the actual measured values. This simulation only simulates a specific region (the case of uniform pore distribution), so the simulation mainly compares the effect of different concentrations of yttrium solution on the diffusion effect. The flexural strength of sintered specimens was tested by ETM105D electronic universal testing machine of

Shenzhen Wance Testing Equipment Co., LTD. China) Three point bending test method was used, and the loading speed was 0.5 mm/min. The bulk density and porosity of the sintered sample were determined by using Archimedes' principle. The precision of the balance (BCE224l-1CCN, Sartorius Scientific Instruments (Beijing Co., LTD., China) was 0.0001 g.

Results and Discussion

Microstructure

COMSOL was used to simulate the temperature distribution after holding at temperature for 2 h, during the 600 ℃ debinding process and 1250 ℃ sintering process respectively, and the results are shown in Fig. 1. The sample density was obtained from actual measurements (bulk density of 1.61 g/cm^3, open porosity of 31.55 vol%), and other parameters were obtained by using the built-in material library of the software. The color in the figure represents the temperature, and the closer the color is to red, the higher the temperature. In both cases, the color distribution is uniform and the overall color is consistent, indicating that the sample temperature distribution in these conditions is rather well uniform, and therefore sintering conditions in each area of the sample are similar.

In Fig. 3(a), the phase composition of yttrium-silica coatings with different silica sol contents after sintering is characterized. The XRD spectrum shows the diffraction peak corresponding to yttrium, and there are no other crystal phases. Fig. 3(b) shows the XRD spectra of the coating after heat treatment at high temperature. By comparing the two figures, it can be observed that the yttrium diffraction peak disappears after the simulation casting treatment. This is because yttrium and silica undergo a chemical reaction at temperatures ranging from 1000 °C to 1600 °C to form yttrium silicate [35]. As the content of silica sol increases, the yttrium silicate diffraction peak becomes stronger, indicating that a greater amount of yttrium silicate has been formed [36].

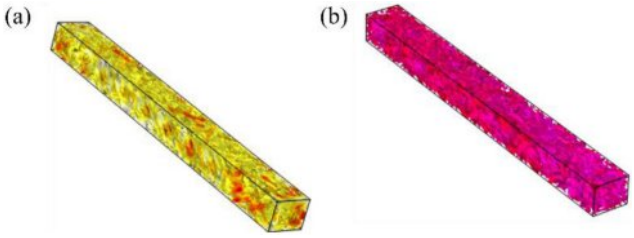

Fig. 1. Temperature distribution of the sample after 2h holding at: (a) 600 ℃; (b) 1250 ℃.

Fig. 3 shows the microstructure of silica samples impregnated with YCl_3 solutions of different concentrations (0.010, 0.020, 0.030 mol/L). Fig. 3(a) shows the sample obtained when YCl_3 concentration was 0.01 mol/L; it is observed that the sample has narrow cracks and many pores. When the concentration increased to 0.020 mol/L, as shown in Fig. 3(b), the cracks of the sample were significantly reduced, and the number of pores was also reduced. When the concentration rose to 0.03 mol/L, as shown in Fig. 3(c), the number of cracks and pores increased. It can be observed, therefore, that with the increase of YCl_3 concentration, the cracks and pores of the sample first decrease and then increase.

The YCl_3 solution not only added Y^{3+} into the silica ceramic, but also added Cl^- into the inside of the sample, so the observed microstructural changes are caused by the joint action of Y^{3+} and Cl^-. Fig. 3 shows the micromorphology of a silica sample with the change of yttrium chloride concentration. Y^{3+} can promote the crystallization and growth of silica, improve the density and increase the strength.

This means that when the concentration is low (0.010 to 0.020 mol/L), Y^{3+} play a leading role in promoting the crystallization of silica, and the increase of solution concentration has a significant improvement effect on silica ceramics in general. When the concentration is high (0.020 to 0.030 mol/L), the damage of Cl^- to silica exceeded the improvement brought by the increase of yttrium ion concentration. Beniaiche et al. [38].

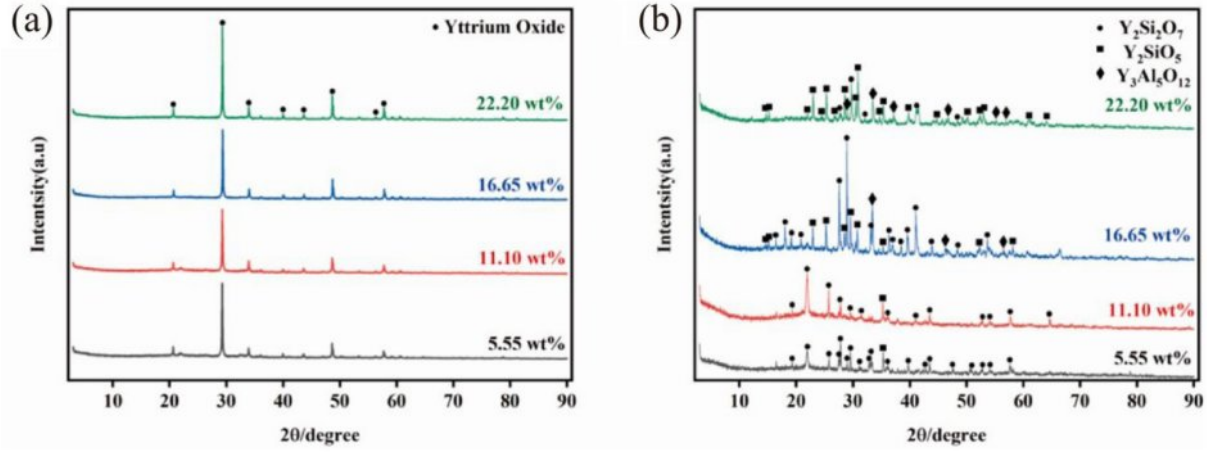

Fig. 2. [36]. XRD patterns of inert coatings with different silica sol content (a) after sintering and (b) after impregnation treatment

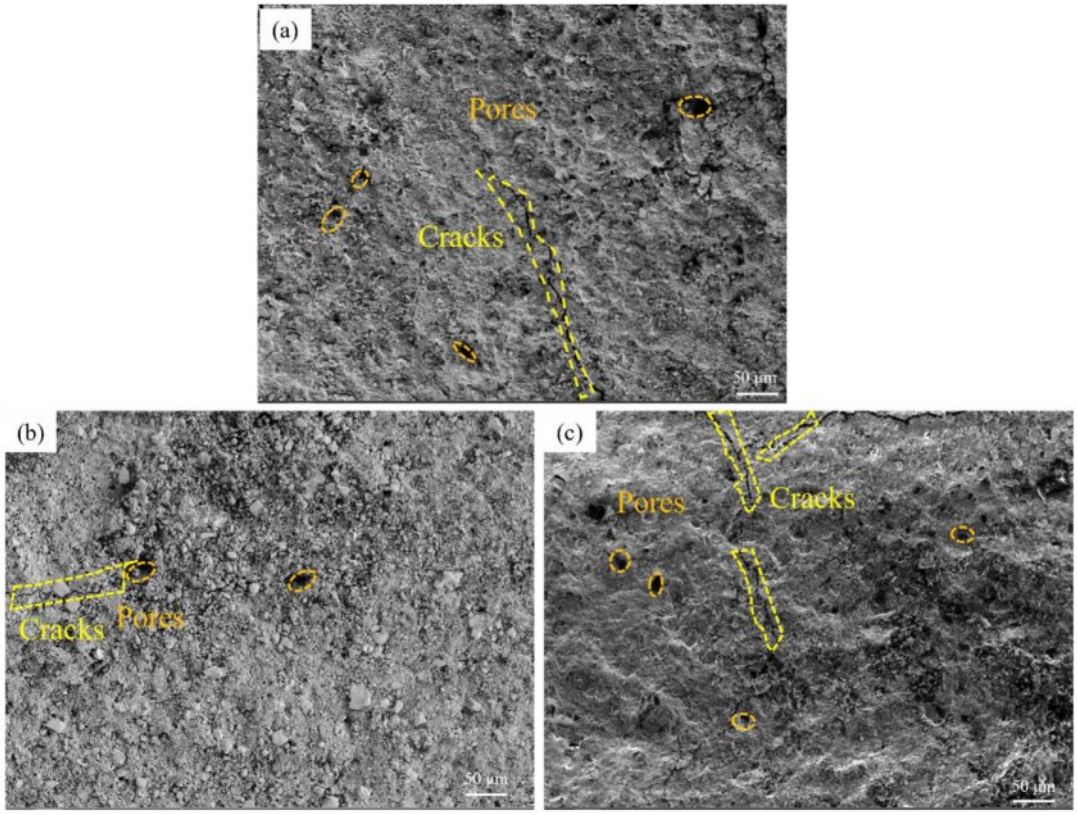

Fig. 3. Microstructure of samples impregnated with YCl_3 solutions of different concentration: (a) 0.010 mol/L; (b) 0.020 mol/L; (c) 0.030 mol/L.

investigated the effects of different concentrations of Y_2O_3 on the surface and volume crystallization of multi-component silicate glass. The results indicated that the addition of Y_2O_3 significantly altered the crystalline phase and crystallization process of the glass. The research also indicates that Y^{3+}, by altering the network structure, reduce the activation energy of crystallization, thereby promoting crystallization and significantly enhancing the nucleation rate and crystallization rate of the crystal phase [39, 40].

Fig. 4 shows the high resolution images of the microstructure of ceramic samples impregnated with different concentrations (0.010, 0.020, 0.030 mol/L) of YCl_3 solution. Fig. 4(a) shows a sample impregnated with a solution of concentration 0.010 mol/L, and there are very large cracks and pores between the grains. Fig. 4(b) shows that when the solution concentration was 0.020 mol/L, the size of cracks and pores between grains was reduced to a large extent. This confirms the above statement. The increase in Y^{3+} concentration does indeed promote the nucleation and growth of grains and the densification of ceramics. The increase of cracks and pores was observed in Fig. 3(c), but this phenomenon was not observed in Fig. 4(c). Therefore, the increase of cracks and pores was not caused by the change of sintering effect. Ding et al[41]. analyzed and studied the reaction of SiC composites with molten chloride mixtures at 700 ºC through SEM and EDX, and found that the molten salt would react with silicon. However, unlike the uniform and flat corrosion in the alloy, the corrosion would lead to the appearance of pores or cracks near SiC and free silicon.

Unlike Cl^-, $Y(NO_3)_3$ has been proved to be a suitable sintering agent capable of improving the sintering of ceramics, but unlike this study, previous studies usually investigated its use with ceramic powders [42-44]. Fig. 5 shows the microstructure of ceramic samples impregnated with different concentrations (0.010, 0.020, 0.030 mol/L) of $Y(NO_3)_3$ solution after sintering. Fig. 5(a) shows the sintered microstructure of an impregnated sample with a $Y(NO_3)_3$ concentration of 0.010 mol/L. A long crack can be observed in the image. The strength of the sample is low, and it is easy to crack in advance. When the concentration is increased to 0.020 mol/L(Fig. 5(b)), no cracks can be observed in the figure, only many small pores. When the concentration continues to increase to 0.030 mol/L (Fig. 5(c)), only a tiny crack can be observed in the sample. The results indicated that, with the increase of $Y(NO_3)_3$ concentration in the solution, the densification of ceramics was improved and the macroscopic defects disappeared.

The microstructure of the samples was observed under high-resolution SEM, as shown in Fig. 6. Fig. 6(a) shows the sample impregnated with a solution with a $Y(NO_3)_3$

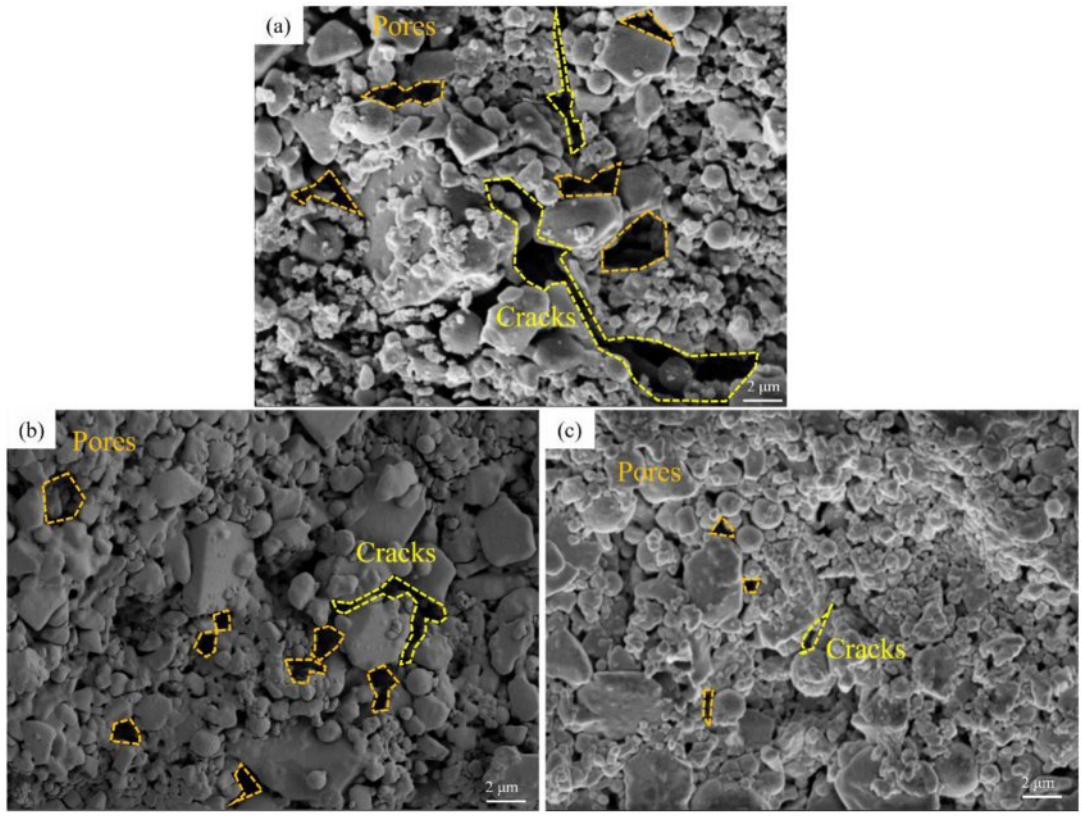

Fig. 4. Microstructure of samples impregnated with YCl_3 solutions of different concentration: (a) 0.010 mol/L; (b) 0.020 mol/L; (c) 0.030 mol/L.

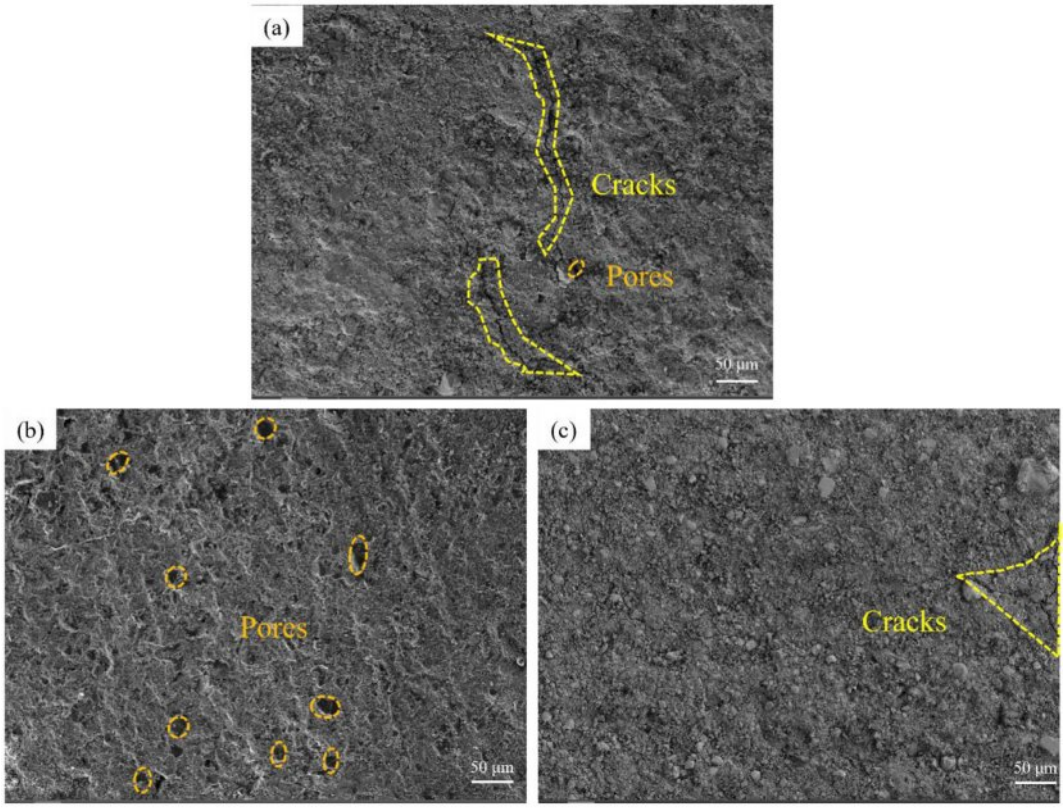

Fig. 5. Microstructure of samples impregnated with $Y(NO_3)_3$ solutions of different concentration: (a) 0.010 mol/L; (b) 0.020 mol/L; (c) 0.030 mol/L.

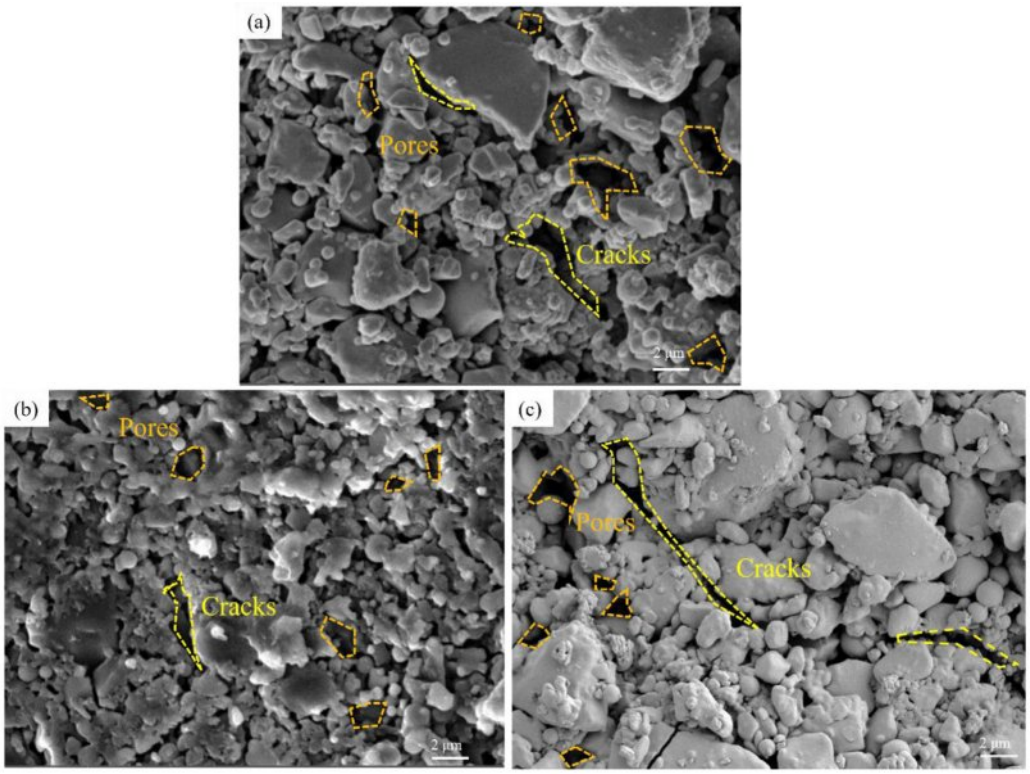

Fig. 6. High resolution images of the microstructure of samples impregnated with $Y(NO_3)_3$ solutions of different concentration: (a) 0.010 mol/L; (b) 0.020 mol/L; (c) 0.030 mol/L.

concentration of 0.010 mol/L, and large cracks and pores can be observed. Fig. 6(b) shows the sample impregnated with a solution concentration of 0.020 mol/L, where pore and crack size decrease. The sample crack width in Fig. 6(c) is already very small, and small cracks are conducive to consuming the energy of major cracks during the fracture process, delaying crack propagation and fracture occurrence, and improving the mechanical properties of the material. Fig. 5 and Fig. 6 show that the increase of $Y(NO_3)_3$ concentration was positively correlated with the improvement of microstructure of silica ceramic samples. Compared with the samples vacuum impregnated with YCl_3, the samples impregnated with $Y(NO_3)_3$ achieved better sintering and have higher strength (see later).

In order to compare the degree of improvement in sintering of the two impregnating solutions, the pore size was digitally measured in the high-resolution SEM images, and the results are shown in Fig. 7. It can be observed that the pore diameter decreases with the increase of solution concentration, and the pore diameter of the sample impregnated by a $Y(NO_3)_3$ solution was smaller than that of the sample impregnated by a YCl_3 solution at the same concentration. With the increase of concentration, the pore diameter of the sample impregnated with the $Y(NO_3)_3$ solution decreased significantly. When the concentration increased from 0.010 mol/L to 0.030 mol/L, the pore diameter decreased by 25.58% (from 0.86 ± 0.04 μm to 0.64 ± 0.02 μm). When the concentration of YCl_3 solution increased from 0.010 mol/L to 0.030 mol/L, the diameter of the pores in the impregnated sample changed by only 12.37% (from 0.91 ± 0.06 μm to 0.79 ± 0.03 μm). Moreover, the pore diameter of samples infiltrated with YCl_3 solutions with a concentration of 0.020 mol/L was 0.82 ± 0.04 μm, showing little change compared with that of a YCl_3

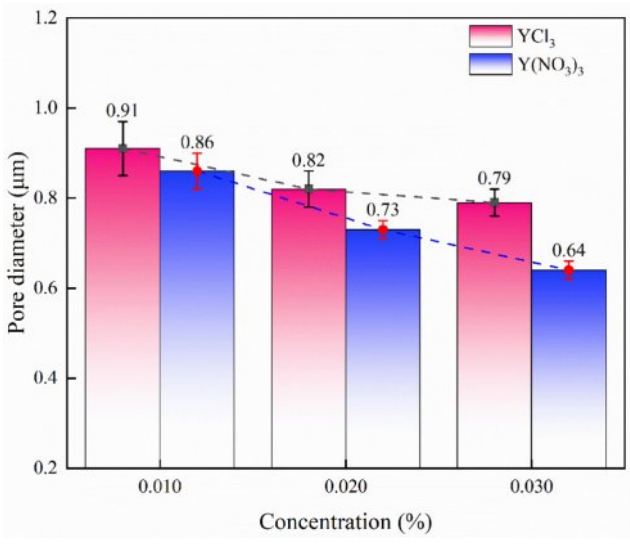

Fig. 7. Diameter of the pores in samples impregnated with solutions of different concentrations of YCl_3 and $Y(NO_3)_3$.

solution with a concentration of 0.030 mol/L (0.79 ± 0.03 μm).

This confirms the above statement that samples impregnated with $Y(NO_3)_3$ solution have better sintering characteristics, and the improvement of sample sintering is positively correlated with the concentration of $Y(NO_3)_3$ in the solution. With the increase of YCl_3 solution concentration, the concentration of Y^{3+} and Cl^- increase synchronously. Under the condition of higher concentration, Cl^- has an obvious damage effect on the samples.

The diffusion of yttrium in silicon samples during the sintering process of impregnated silicon samples was simulated by using COMSOL software. A porous medium model was established in the COMSOL software to simulate the diffusion of yttrium at different concentrations. To more clearly explore the influence of different concentrations of impregnating solutions on the impregnation process, the only variable for simulation was the different concentrations of the impregnating solutions. Studies have shown that in the low concentration range (<0.1 mol/L), the diffusion coefficient changes less with the increase of concentration [45]. Therefore, the diffusion coefficients of this simulation are all consistent, ignoring the slight differences caused by different concentrations. The remaining parameters are all from the material library that comes with the COMSOL software.Based on the study of Nazyrov et al. [44]., $D=2.0310^{-12}$ was selected as the diffusion coefficient. For other material parameters, the software built-in database was used. Fig. 8 is a simulation diagram of yttrium diffusion after sintering of samples impregnated with yttrium solution of different concentrations (concentration=0.005, 0.010, 0.015, 0.020, 0.025, 0.030%). The viewing angle is the viewing angle of the upward view, that is, the viewing surface is the contact surface with the build platform. The color in the figure represents the concentration of yttrium, the closer the color is to red, the higher the concentration, and the closer the color is to blue, the lower the concentration. It can be observed that the yttrium element has a limited diffusion depth inside the silica sintered sample, and the closer to the core, the less yttrium element content. As expected, the higher the concentration of yttrium solution, the higher the concentration of yttrium element impregnating the sample, and the deeper the diffusion.

Physical properties

The bulk density and porosity of the sample were measured by the Archimedes' method. The results for the samples impregnated with $Y(NO_3)_3$ solutions of different concentration are shown in Fig. 9. We can observe that, with the increase of the concentration of $Y(NO_3)_3$, the density presents a linearly increasing trend, while the porosity shows a decreasing trend with increasing $Y(NO_3)_3$ concentration. When the concentration of $Y(NO_3)_3$ increased from 0.005 mol/L to 0.030 mol/L, the bulk density increased 4.87% by 0.074 g/cm^3 (from 1.518 ± 0.005 g/cm^3 to 1.592 ± 0.006 g/cm^3), while the open

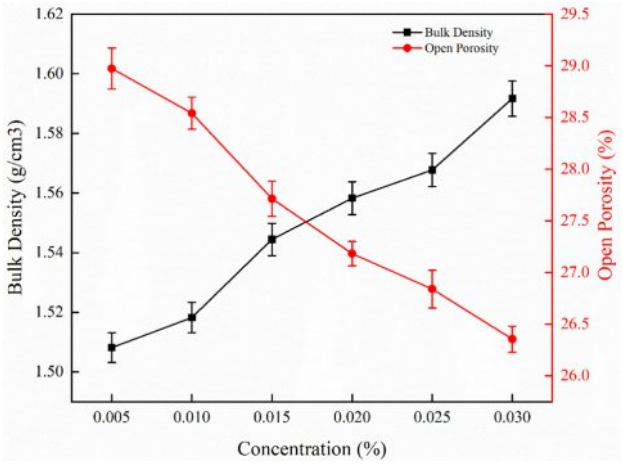

Fig. 9. Bulk density and porosity of samples impregnated with $Y(NO_3)_3$ solutions of different concentration.

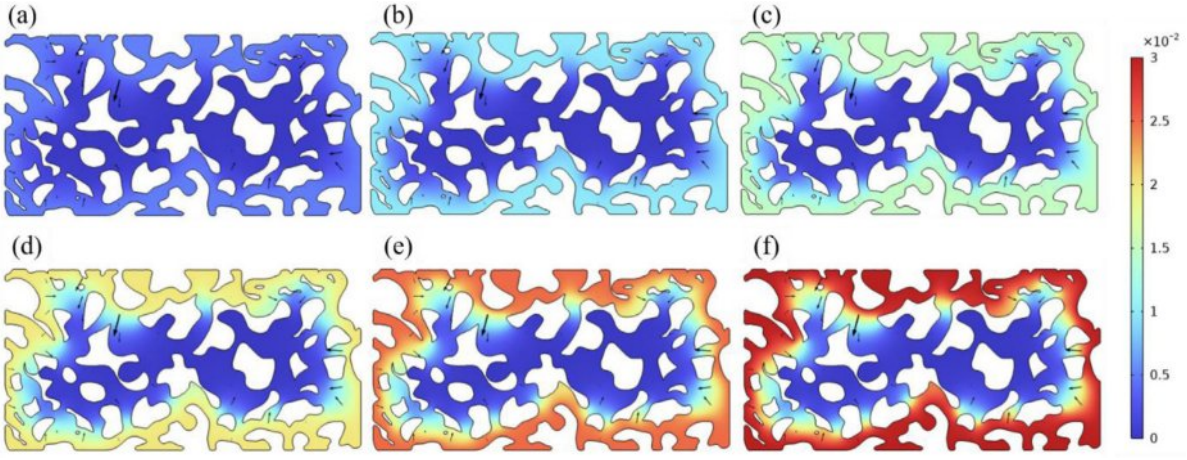

Fig. 8. Simulation of the diffusion into sintered samples of solutions with different yttrium concentration: (a) 0.005 mol/L; (b) 0.010 mol/L; (c) 0.015 mol/L; (d) 0.020 mol/L; (e) 0.025 mol/L; (f) 0.030 mol/L.

porosity decreased by only 2.19% (from 28.54 ± 0.16 vol% to 26.35 ± 0.13 vol%). The density of the samples was successfully increased with limited reduction in porosity. Consistent with the conclusions in Fig. 5, Fig. 6 and Fig. 7, the densification of ceramics was improved with the increase of $Y(NO_3)_3$ concentration, with yttrium promoting the growth of crystals and reducing the defects in the microstructure. However, since the yttrium was added by dipping in this study, and the solution concentration was low, the observed effects concerning the sample density are not very strong. Beniaiche et al. [38]. discovered through XRD experiments and FTIR spectra experiments in multi-component silicate glass, they found that the higher the concentration of Y_2O_3 leading to the higher the degree of crystallization. They attributed this to that the Y_2O_3 acting as a network modifier, effectively increasing the frequency of Si-O-X bonds and enhancing the bonding strength of atoms in the crystalline phase of the material.

The results for samples impregnated with YCl_3 solutions of different concentrations are shown in Fig. 10. When yttrium concentration increased from 0.005 mol/L to 0.030 mol/L, the bulk density increased 3.62% by 0.055 g/cm^3 (from 1.521 ± 0.004 g/cm^3 to 1.576 ± 0.005 g/cm^3), and the porosity decreased by 2.02% (from 28.59 ± 0.13% to 26.57 ± 0.14%). The sintering densification for the samples impregnated with YCl_3 was lower than that observed for samples impregnated with $Y(NO_3)_3$. This difference is caused by the difference between nitrate and chloride ions. NO_3^- is not thought to affect silica directly, but indirectly by affecting the system environment [47]. As shown in Fig. 3 and Fig. 4, when the concentration of YCl_3 solution was increased to 0.020 mol/L, the densification of the samples improved, but when the concentration increased to 0.030 mol/L, many pores and cracks appeared in the microstructure of the sample. Therefore, with the increase of the concentration of the solution, the increase of the concentration of ionized ions increased the difference between the two solutions, resulting in different properties.

Fig. 11 shows the flexural strength of samples impregnated with solutions with different concentrations of $Y(NO_3)_3$ and YCl_3. With the increase of the concentration, the strength of the impregnated samples increased to different degrees depending on the type of solution used. When the concentration increased from 0.005 mol/L to 0.030 mol/L, the strength of the sample impregnated with $Y(NO_3)_3$ solution increased by 56.60% (from 2.88 ± 0.13 MPa to 4.51 ± 0.15 MPa). When the concentration increased from 0.005 mol/L to 0.030 mol/L, the strength of the sample impregnated with YCl_3 solution increased by 57.14% (from 2.24 ± 0.17 MPa to 3.52 ± 0.18 MPa). The strength of samples impregnated with $Y(NO_3)_3$ solution and YCl_3 solution was the highest at the highest concentration (0.030 mol/L).

From the point of view of the percentage of increase in strength with the increase of the concentration of the solutions, the trend for the two solutions was similar. However, when the concentration of YCl_3 impregnated samples increased from 0.025 mol/L (3.51 ± 0.13 MPa) to 0.030 mol/L (3.52 ± 0.18 MPa), there was almost no change in strength. The strength of the sample impregnated with $Y(NO_3)_3$ was always about 0.6 MPa higher than that of the sample impregnated with YCl_3 at the same concentration. In general, the flexural strength is positively correlated with the bulk density and negatively correlated with the porosity. The dense microstructure is conducive to providing a larger force area when bearing loads, and fewer defects can reduce the probability of premature fracture of the sample. By comparing the microstructure in Fig. 3 and Fig. 5, the $Y(NO_3)_3$ impregnated samples had a denser microstructure, and higher bulk density is confirmed in Fig. 9 and Fig. 10. Moreover, the number of pores and cracks in the micromorphology of the sample impregnated with

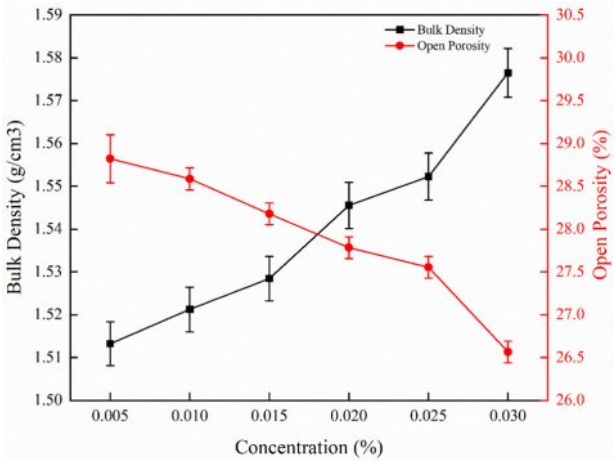

Fig. 10. Bulk density and porosity of samples impregnated with YCl_3 solutions of different concentration.

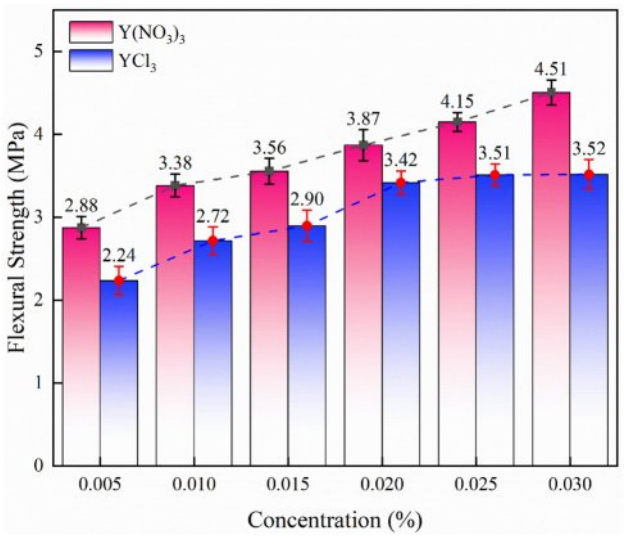

Fig. 11. Flexural strength of samples impregnated with solution with different concentration of YCl_3 and $Y(NO_3)_3$.

0.030 mol/L YCl_3 increased, which led to the decline of the mechanical properties of the sample. Despite the concentration of yttrium ions increasing, the strength of the sample still could not be improved.

Dimensional accuracy

The shrinkage rate of the sintered samples is related to the solid content, porosity and density after sintering. Due to the anisotropy of 3D printed ceramics, the shrinkage rate of the samples in different directions is significantly different [48-51]. The shrinkage in the length direction and the width direction is mainly related to the structure density caused by the intra-layer particle rearrangement, while the shrinkage in the height direction is mainly caused by the intra-layer and inter-layer particle rearrangement. Therefore, the height direction usually has a higher shrinkage rate.

As shown in Fig. 9, the densification of the samples was improved by immersion with $Y(NO_3)_3$ solution. By measuring the sample size, the shrinkage rate of the impregnated sample with yttrium nitrate solution of different concentrations was obtained, as shown in Fig. 12. With the increase of $Y(NO_3)_3$ concentration (from 0.005 mol/L to 0.030 mol/L), the shrinkage rate in different directions increased. The linear shrinkage in the length direction increased by 65.11% (from 2.78 ± 0.12% to 4.59 ± 0.15%), the shrinkage in the width direction increased by 119.37% (from 2.84 ± 0.13% to 6.23 ± 0.16%), and the shrinkage in the height direction increased by 42.91% (from 2.96 ± 0.13% to 4.23 ± 0.14%). Therefore, it is confirmed that the $Y(NO_3)_3$ solution greatly promotes the sintering densification of the samples.

The values of the linear shrinkage after sintering of the samples impregnated with solutions with different concentrations of yttrium chloride are shown in Fig. 13.

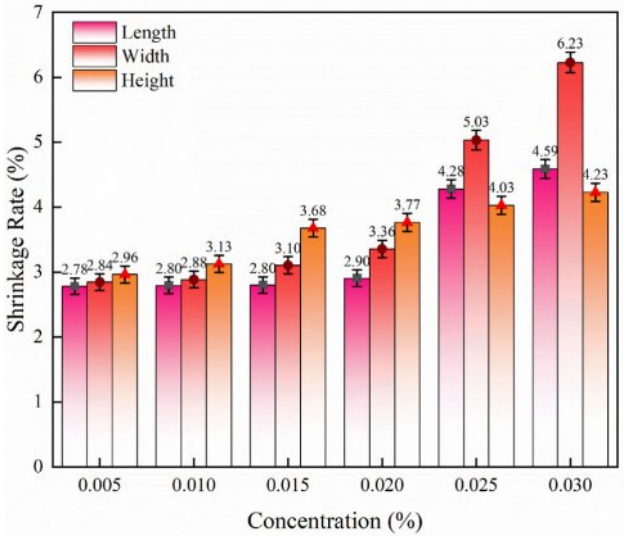

Fig. 12. Linear shrinkage of samples impregnated with $Y(NO_3)_3$ solutions of different concentration.

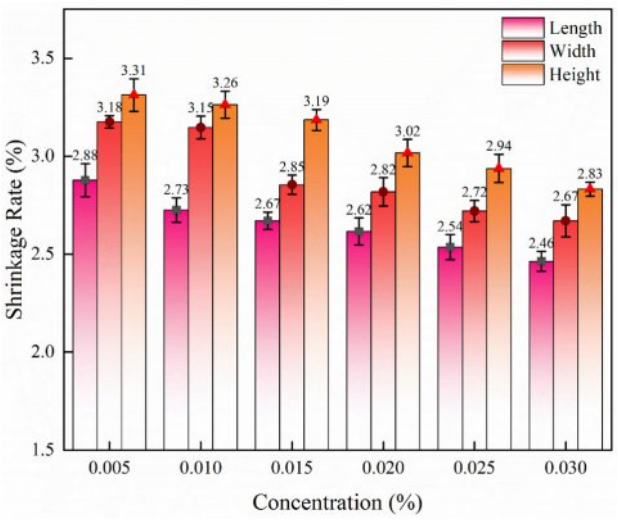

Fig. 13. Linear shrinkage of samples impregnated with YCl_3 solutions of different concentration.

Surprisingly, with the increase in YCl_3 concentration, the shrinkage of the samples decreased. With the increase in YCl_3 concentration (0.005 mol/L to 0.030 mol/L), the shrinkage in the length direction decreased by 14.58% (from 2.88 ± 0.08% to 2.46 ± 0.05%), the shrinkage in the width direction decreased by 16.04% (from 3.18 ± 0.03% to 2.67 ± 0.08%), and the shrinkage in the height direction decreased by 14.50% (from 3.31 ± 0.08% to 2.83 ± 0.04%). A large number of studies have shown that yttrium is easily enriched at grain boundaries [32, 52-56]. In the microstructure images of Fig. 3 and Fig. 4, the YCl_3 solution impregnated sample showed many cracks and pores. The decrease in shrinkage of YCl_3 samples may be caused by the increase in the number of cracks and pores. As the concentration of yttrium chloride increases, the concentration of chloride ions also increases, and the defects of silica increase, and the increase of yttrium elements cannot completely offset this negative effect. In the sintering process, although the degree of densification is increased, the grain nucleation and growth are hindered resulting in a decrease in the shrinkage in terms of dimensional accuracy [57].

Conclusions

In this study, vacuum impregnation was used to modify 3D printed silica ceramics, and the effects of concentrations of yttrium nitrate and YCl_3 on their properties were studied. The degree of sintering was improved by impregnating with an yttrium-containing solution. While maintaining a desired amount of porosity, the mechanical properties of the parts were enhanced. However, the Cl^- in YCl_3 solution lead to defects in silica, forming cracks and pores, which hinder the viscous flow, reduce the densification degree and decrease the flexural strength in the samples. Therefore, using the highest concentration (0.030 mol/L) of $Y(NO_3)_3$ solution

is the best choice for vacuum impregnation of 3D printed silica ceramics, resulting in samples with optimal microstructure and the best mechanical properties. The open porosity was 26.35 ± 0.13%, the shrinkage 4.59 ± 0.15%, the bulk density 1.592 ± 0.006 g/cm^3, and the flexural strength at room temperature 4.51 ± 0.15 MPa.

Declaration of Competing Interest

The authors declare that they have no known competing financial interests or personal relationships that could have influenced the work reported in this paper.

Acknowledgements

This work was sponsored by Natural Science Foundation of Xinjiang Uygur Autonomous Region (2023D01C192), the Xinjiang Tianchi Talent Introduction Plan (51052300585), and the Fundamental Research Funds for Autonomous Region Universities (XJEDU2022P002).

References

1. X. Wang, Y. Zhou, L. Zhou, X. Xu, S. Niu, X. Li, and X. Chen, J. Eur. Ceram. Soc. 41[8] (2021) 4650-4657.
2. Youna Lim, Seunggu Kang, and Kangduk Kim, J. Ceram. Process. Res. 25 (2024) 673-682
3. M. Huo, Q. Li, X. Yue, J. Liang, and J. Li, Ceram. Int. 50[11] (2024) 20644-20653.
4. Z. Chen, X. Sun, Y. Shang, K. Xiong, Z. of A. on C.C. and P. of S.-B.C.C. Xu, R. Guo, S. Cai, and C. Zheng, J. Adv. Ceram. 10[2] (2021) 195-218.
5. H. Li, Y. Liu, Y. Liu, J. Wang, and Z. Lu, 3D Print. Addit. Manuf. 7[1] (2020) 8-18.
6. G. Moulika and P. Ponnusamy, J. Ceram. Process Res. 23(2022) 391-396.
7. S. Zakeri, M. Vippola, and E. Levänen, Addit. Manuf. 35 (2020) 101177.
8. T. Lin, T. Bai, H. Shao, Y. Dong, and M. Fan, Int. J. Refract. Met. Hard Mater. 119 (2024) 106505.
9. D. Zhao, H. Su K. Hu, Z. Lu, W. Zhang, and X Li, J. Addit. Manuf. 52 (2022) 102650.
10. X. Wang, M. Jiang, Z. Zhou, J. Gou, and D. Hui, Compos. Part B Eng. 110 (2017) 442-458.
11. S.E. Efrat, S. Yaelle, M.Y. Moshkovitz, L.K. Yael, and R. Uri, J. Nano Letters. 20 (2020) 6598-6605.
12. W. Zheng, J.-M. Wu, S. Chen, K.-B. Yu, S.-B. Hua, C.-H. Li, J.-X. Zhang, and Y.-S. Shi, J. Addit. Manuf. 48 (2021) 102396.
13. J. Zhang, G. Zhang, J. Song, F. Yu, N.H. Wong, J. Sunarso, N. Yang, B. Meng, X. Tan, and S. Liu, J. Addit. Manuf. 80 (2024) 103983.
14. T. Sivarupan, N. Balasubramani, P. Saxena, D. Nagarajan, and M.S. Dargusch, Addit. Manuf. 40[12] (2021) 101889.
15. X. Li, L. Yan, A. Guo, H. Du, F. Hou, and J. Liu, Ceram. Int. 50[19] (2024) 35609-35614.
16. S.E. Amrani, M. Sun, S. Valdueza-Felip, F.B. Naranjo, M.R. Britel, M. Ferrari, and A. Bouajaj, Ceram. Int. 51 (2024) 16786-16790.
17. C. Qian, K. Hu, Z. Shen, et al. Ceram. Int. 49 (2023) 17506-17523.
18. K. Eltayeb, W. Hong, F. Chen, Y.-H. Han, Q. Shen, and L. Zhang, J. Ceram. Process. Res. 18 (2017) 1-9.
19. N.G. Kottke, M. Tajmar, and F.G. Hey, Vacuum 220 (2024) 112812.
20. J. Zhang, J.-M. Wu, H. Liu, W. Zheng, C.-S. Ye, S.-F. Wen, C.-Z. Yan, and Y.-S. Shi, J. Mater. Sci. Technol. 157 (2023) 71-79.
21. H. Liu, R.-Z. Zhang, J.-M. Wu, W.-K. Li, S.-X. Zhou, J. Zhang, W. Zheng, C.-Z. Yan, S.-F. Wen, C.-S. Ye, Y.-S. Shi, C.-Y. Chen, and Z.-M. Ren, Addit. Manuf. 95 (2024) 104527.
22. J.A.B. Pérez, E.R. Morales, F.P. Delgado, C.A.M. Avendaño, E.M.A. Guzman, and N.R. Mathews, Vacuum. 215 (2023) 112276.
23. E. Betoret, N. Betoret, P. Rocculi, and M.D. Rosa, Trends Food Sci. Technol. 46[1] (2015) 1-12.
24. M. Li, C. Fang, Y. Cheng, X. Zhang, H. Han, J. Zhao, and Y. Zhang, Vacuum 221 (2024) 112885.
25. H. Liu, C. Liu, Y. Sui, Z. Liu, T. Zhang, Z. Zhang, S. Sun, and J. Jia, Vacuum 220 (2024) 112732.
26. H. Li, Y. Huang, and P. Colombo, Ceram. Int. 51[5] (2025) 6309-6318.
27. Y. Huang, H. Li, and P. Colombo, Silicon 17[3] (2024) 487-498.
28. Zhili Cuia, Shiming Xiaob, Xianli Luob, et al., J. Ceram. Process. Res. 24[5] (2023) 835-840.
29. C.-W. Kuo, Y.-H. Shen, I.-M. Hung, S.-B. Wen, H.-E. Lee, and M.-C. Wang, J. Alloys Compd. 472[1] (2009) 186-193.
30. J.-W. Huang, X.-A. Lv, X.-F. Dong, X.-N. Ren, and C.-C. Ge, Ceram. Int. 50[13] (2024) 24734-24742.
31. J.-M. Zhang, X.-W. Chen, X. You, Q.-G. Li, M.-M. Wang, X.-Y. Zhang, Y.-M. Kan, Y.-D. Xue, and S.-M. Dong, S Corros. Sci. 249 (2025) 112848.
32. H. Yu, R. Kasada, K. Inoue, S. Kondo, Y. Ogino, and S. Ukai, Corros. Sci. 227 (2024) 111775.
33. X. Cheng, C. Deng, X. Deng, X. Wang, J. Ding, Z. Liu, B. Ma, Z. Wang, H. Zhu, and C. Yu, J. Eur. Ceram. Soc. 45[5] (2025) 117116.
34. H. Li, Y. Huang, and P. Colombo, Mater. Today Commun. 41 (2024) 110616.
35. A.H. Haritha and R.R. Ramachandra, Ceram. Int. 45 (2019) 24957-24964.
36. A.R. Wang, X. Li, Y.K. Yang, S.X. Niu, and J. Li, Ceram. Int. 40 (2025) 0272-8842.
37. T.H. Ho, T.H. Do, H.D. Tong, E.J. Meijer, and T.T. Trinh, J. Phys. Chem. B 127[36] (2023) 7748-7757.
38. A. Beniaiche, A. Tamayo, N. Belkhir, F. Rubio, and A. Chorfa, J. Rubio, Crystals 14[3] (2024) 214.
39. Q. Zheng, Y. Liu, M. Li, Z. Liu, Y. Hu, X. Zhang, W. Deng, and M. Wang, J. Eur. Ceram. Soc. 40[2] (2020) 463-471.
40. P. Vomacka, O. Babushkin, J. Eur. Ceram. Soc. 15[9] (1995) 921-928.
41. W. Ding, Y. Shi, F. Kessel, D. Koch, T. Bauer, Npj Mater. Degrad. 3[1] (2019) 42.
42. Y. Qi, H. Wu, W. Zhang, P. Huang, X. Chen, K. Lin, and S. Wu, J. Eur. Ceram. Soc. 45[7] (2025) 117228.
43. L. Lin, H. Wu, K. Lin, Y. Li, P. Ni, D. Lu, P. Sheng, and S. Wu, Addit. Manuf. 84 (2024) 104115.
44. P. Sheng, G. Nie, Y. Li, L. Wang, J. Chen, X. Deng, and S. Wu, Addit. Manuf. 74 (2023) 103732.
45. Muhammed J. Kadhim, and M.I. Gamaj, Iraqi J. Phys. 18[46] (2020) 2028.
46. D. Nazyrov, M.I. Bazarbaev, and A.A. Iminov, Semiconductors 40[7] (2006) 768-769.

47. J. Wang and S. Wang, Chem. Eng. J. 411 (2021) 128392.
48. Z. Zhao, X. Liang, Y. Li, Q. Wang, L. Pan, and S. Sang, J. Eur. Ceram. Soc. 44[11] (2024) 6651-6659.
49. S. Niu, K. Wang, Y. Luo, Y. Yang, Y. Zhou, Y. Si, X. Li, and X. Xu, Ceram. Int. 50[14] (2024) 25886-25894.
50. J.Y. Wang, S.R. Sama, P.C. Lynch, and M.R. Guha, Procedia Manufacturing. 34 (2019) 683-694.
51. C. Manière, G. Kerbart, C. Harnois, and S. Marinel, Acta Mater. 182 (2020) 163-171.
52. X. Li, D. Yang, Z. Zhao, F. Li, and Y. Zhang, Ceram. Int. 51 (2025) 22153-22161.
53. S. Zhang, F. Li, Y. Xie, Z. Li, Y. Wang, S. He, and B. Liu, J. Alloys Compd. 1022 (2025) 179949.
54. B. Liu, C. Yuan, W. Zhao, X. Zhang, and L. Zeng, Ceram. Int. 51[6] (2025) 8116-8128.
55. G. Zhang, W. Liu, H. Bian, W. Xi, Y. Zao, K. Zhang, and H. Wang, Surf. Coat. Technol. 503 (2025) 132025.
56. C. Grimme, K. Ma, R. Kupec, C. Oskay, E.M.H. White, A.J. Knowles, and M.C. Galetz, Surf. Coat. Technol. 485 (2024) 130891.
57. W. Duan, Z. Yang, D. Cai, J. Zhang, B. Niu, D. Jia, and Y. Zhou, Ceram. Int. 46[4] (2020) 5132-5140.